

# Using a Periodic Square Wave Test Signal to Detect Crosstalk Faults

Ming Shae Wu and Chung Len Lee

National Chiao Tung University

This BIST scheme simplifies the detection of crosstalk faults in deep-submicron VLSI circuits in the boundary scan environment. Simulation results show that with just a few random patterns, fault coverage for most large benchmark circuits can exceed 90%.

**DEEP-SUBMICRON TECHNOLOGY'S** advanced high-density and high-speed VLSI has reduced distances between wires and devices. Perhaps because of manufacturing defects, parasitic capacitors become important sources of internal circuit noise. In 0.18- $\mu\text{m}$  technology, for example, two parallel lines that are 240  $\mu\text{m}$  long with a spacing of 0.23  $\mu\text{m}$  will produce a 25-fF parasitic capacitance in the normal fabrication condition.<sup>1</sup> A manufacturing defect, such as narrower spacing between two conduction lines, will make the parasitic capacitances even larger. Noise induced by these parasitic elements interferes with normal VLSI operation by generating unexpected pulses, speeding up or slowing down the transition speed on interconnecting (victim) lines when the nearby aggressor line changes state.<sup>2,4</sup> If unexpected pulses appear, and flip-flops catch these pulses during their sampling time, the system will fall into erroneous states. If the slowed-down transitions exceed the flip-flops' clock period, erroneous states also result.

Many researchers have focused on analysis, testing, and reduction of crosstalk faults.<sup>2,10</sup> Chen et al. simply used Kirchoff's voltage law to analyze crosstalk noise with a three-step approach.<sup>2</sup> Lee et al. analyzed crosstalk in both frequency and time domains to gain insight into effects that cause errors.<sup>3</sup> Sabet and Ilponse considered crosstalk on clock or reset lines and contrived a fault simulator to estimate the fault effect and the detectability of crosstalk faults.<sup>4</sup> Others used proposed algorithms to study circuit

timing characteristics.<sup>5,7</sup> Bai et al. proposed an at-speed test technique to detect circuit interconnects' crosstalk faults by generating a six-vector test sequence,<sup>8</sup> and Lai et al. proposed a software-based self-test methodology to detect crosstalk faults on

interconnects.<sup>9</sup> Several researchers used a timing analysis technique to help generate test patterns for crosstalk faults in the desired time window.<sup>5,7,8,10</sup>

Testing for crosstalk faults is difficult because they are pattern dependent and highly unpredictable. Generating test patterns to deterministically detect these faults requires a timing analysis program of high precision, and this takes much computation time. Previously, we proposed a test scheme based on an oscillation square wave signal.<sup>11</sup> If a crosstalk fault between two lines exists, applying the square wave test signal on the aggressor line induces glitches on the victim line that can be detected. This scheme eliminates the need to consider the fault timing issue because any glitches induced (usually unexpectedly) by the crosstalk fault are detectable at the victim line's output.

For the work described in this article, we modified the scheme to test for crosstalk faults of embedded VLSI circuits in the boundary scan environment. The scheme tests for crosstalk faults with a periodic square wave test signal under applied random patterns generated by a linear feedback shift register (LFSR), which is transconfigured from the embedded circuit's boundary scan cells. The scheme simplifies test generation and test application while obviating the fault occurrence timing issue. Experimental results show that coverage for the induced-glitch type of crosstalk fault for large benchmark circuits can easily exceed 90%.<sup>12</sup>

## Circuit-level simulation of induced glitches

Similar studies have investigated induced glitches caused by crosstalk faults,<sup>13</sup> but in our scheme we still do a circuit-level simulation for an aggressor line and a victim line to show the induced glitches at the victim's output. In Figure 1a, a square wave signal constitutes the aggressor line's input, the victim has a static value, and there is a crosstalk fault (the parasitic coupling capacitor between the aggressor and victim lines). The simulated output waveforms at the victim's output E appear in Figure 1b, with those waveforms at A, C, D, and E. The figure shows that for this coupling capacitance value, a periodic pulse train appears at E.

## Test scheme

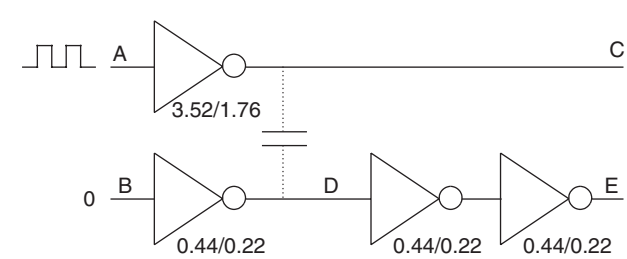
Here we describe the basic idea behind the test scheme and illustrate the test scheme architecture.

### Basic idea

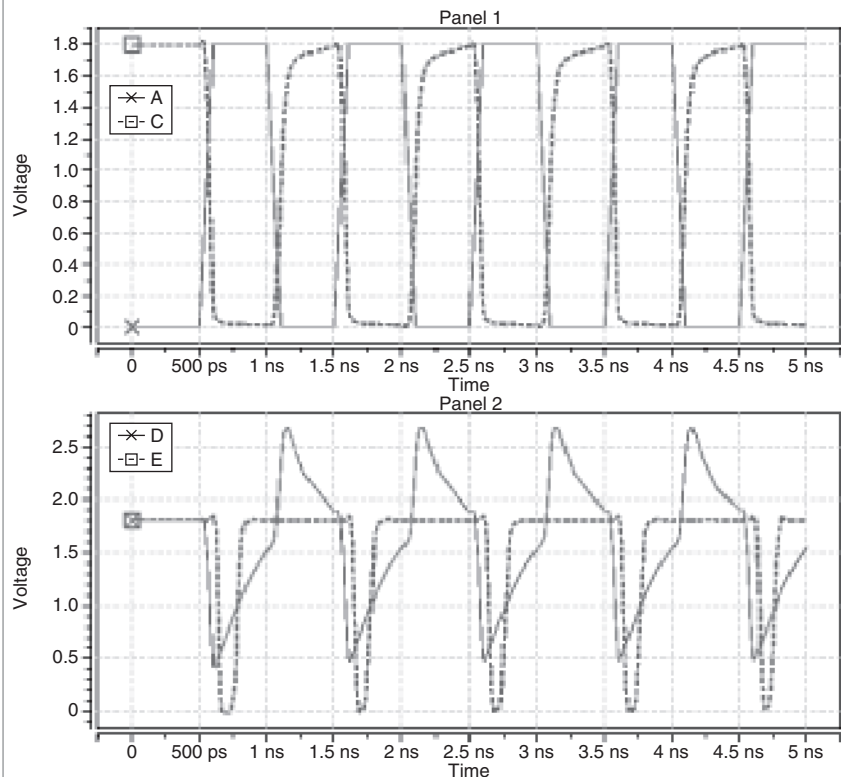
Figure 2 is an example circuit demonstrating the basic idea of how to detect crosstalk faults using the oscillating square wave signal. In the figure,  $I_1, I_2, I_3, I_4,$  and  $I_5$  are inputs;  $O_1, O_2,$  and  $O_3$  are outputs; line A is the aggressor line; line V is the victim line; and the coupling capacitor C represents a coupling fault between lines A and V. When we apply a random test pattern  $\{I, S, I, 0, 0\}$  to the input (where S stands for an oscillating square wave signal), the output will be  $\{O_1, O_2, O_3 = S, 0, I\}$  if the circuit is fault free.  $O_1 = S$  means that an oscillation square wave signal appears at  $O_1$ . However, the existence of coupling fault C between lines A and V will induce a pulse train at line V. The induced pulse train will propagate to output  $O_3$  and be detectable under the applied pattern. Thus, the test has detected coupling fault C.

### Test architecture in a boundary scan environment

Figure 3 shows the test scheme architecture in a boundary scan environment. The input cells store a ran-



(a)



(b)

**Figure 1. Circuit-level simulation for the induced pulses caused by a crosstalk fault. In the simulated circuit, the parasitic coupling capacitance is 25 fF, each driver has a 0.18- $\mu$ m channel length, and the numbers represent the corresponding driver pMOS and nMOS channel width and length ratio of the aggressor and victim lines (a). The input waveform at A produces the simulated waveforms at nodes C, D, and E (b).**

dom pattern generated by an LFSR transformed from boundary scan cells. When testing begins, the tester, under program control, flips the first bit of the input scan cells in polarity and checks all circuit outputs for polarity changes. Any output change, say on output  $O_k$ , indicates a sensitized path between output  $O_k$  and the input. Then the tester applies the oscillating square wave signal S to the input. Pulse trains detected at any output

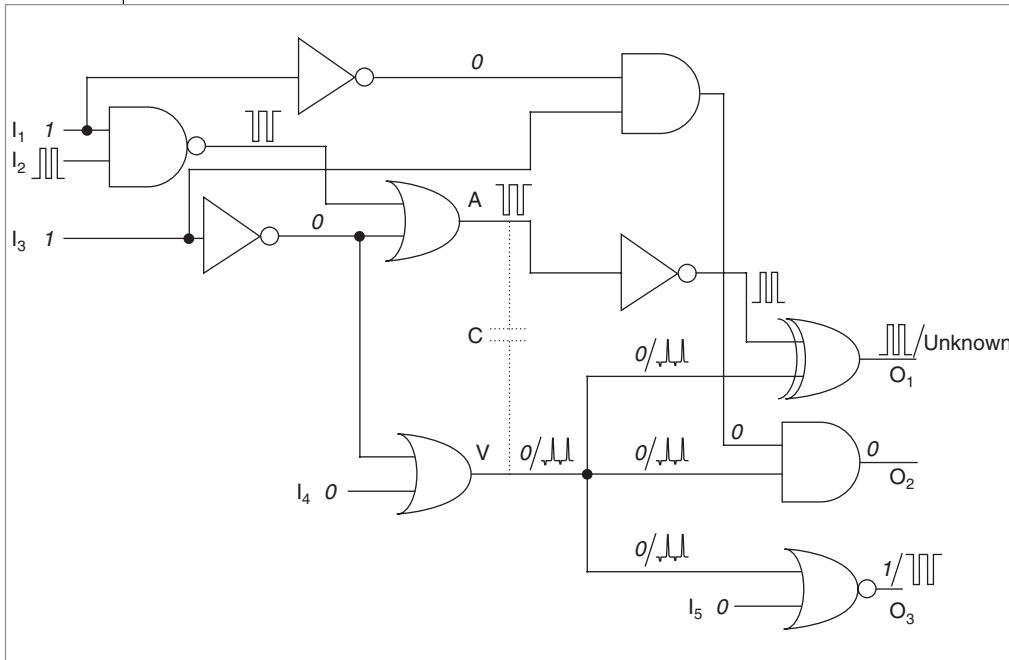


Figure 2. Example circuit demonstrating the test scheme for detecting a crosstalk fault.

quent section, verify.

For the test described, an oscillator (either built in locally or provided by the SoC in which the circuit under test, or CUT, is embedded) can provide the oscillating square wave signal.

### Details of BIST circuits

Here we describe details of the BIST circuits and the boundary scan cell design.

### General description of the circuit

Figure 4 shows the circuit for the BIST architecture in the crosstalk fault

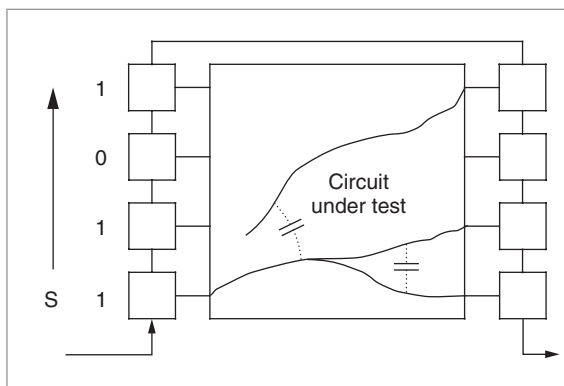


Figure 3. Architecture of the square wave test scheme for crosstalk faults in the boundary scan environment. For one random test pattern applied to the circuit inputs, the tester scans signal S from the inputs' first bit to the last bit.

other than  $O_k$  indicate coupling faults between the sensitized paths and victim lines, and this pattern detects the coupling faults. When this test completes, the same procedure repeats on the second input bit, and so on, for all the remaining input bits. Then the LFSR generates another random pattern and stores it in the input cells, and the test procedure runs again. Applying  $p$  random patterns for  $m$  inputs results in  $m \times p$  tests. Hence, we can expect very high detection efficiency for the patterns, which the experiment's results, discussed in a subse-

detection scheme in greater detail. The circuit contains a random pattern generator block (top) and a detector block (bottom) at the input and output of the CUT, which has  $m$  inputs and  $n$  outputs. The random-pattern generator block contains an  $m$ -bit LFSR, where  $Tclk_0$  is the clock signal that causes the LFSR to change its state and  $Sq$  is the periodic square wave. The shift register's task is to shift a single logic 1 value from its lowest bit to its highest bit. The shift register outputs connect to an  $m$ -bit 2-to-1 multiplexer, whose outputs could be from the LFSR or the  $Sq$ . The detector block contains

- two D-type flip-flops, which are output boundary cells of the CUT and serve to store the test results of the output;
- two exclusive-OR gates ( $XOR_1$  and  $XOR_2$ );
- a detection mode latch (DM), which is enabled by the detection mode latch enable to latch the output of  $XOR_1$ ; and
- an error detector (ED) to detect risky pulses in the output signal.

For one pattern, the circuit has three operational phases: random-test-pattern generation, periodic square wave signal port selection and sensitized-path checking, and square wave test. In the first phase, a pulse arrives at  $Tclk_0$ , and the LFSR changes its state to apply a random pattern to the CUT. The LFSR begins to load

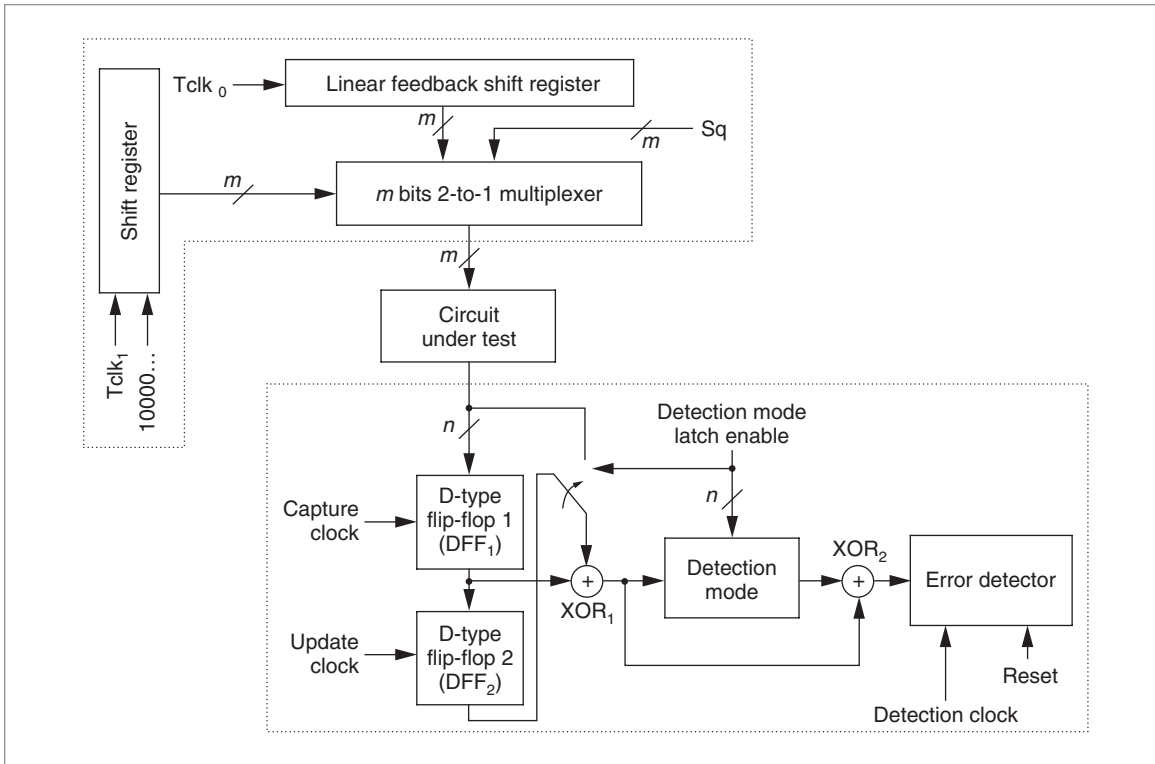


**Figure 4. Circuit detail of the BIST architecture for the crosstalk fault detection scheme.**

logic 1 from its least significant bit (LSB), and the multiplexer selects Sq as its LSB. The second phase identifies the sensitized path, and Sq applies 0 and 1 in sequence to the CUT. The first 0's output result is stored in a D-type positive-edge-triggered flip-flop (DFF<sub>1</sub>), and the output result of the second 1 remains at the CUT output. XOR<sub>1</sub> compares these flop, DFF<sub>1</sub>, and two bits, and its output latches at the DM latch, which the DMLE signal enables at the beginning of this phase. If the DM latch is 1, it means the CUT's output is a sensitized path. In the third phase—square wave test—the tester applies a periodic square wave signal at the rising edge of the test clock to test the circuit. The capture clock (Cap<sub>clk</sub>), the update clock (Update<sub>clk</sub>), and the detection clock (Det<sub>clk</sub>) of the boundary scan cells are synchronized with the test clock. After this phase, the circuit goes back to phase 2 to check another sensitized path because the periodic square wave signal port has been shifted to the second input. Then it returns

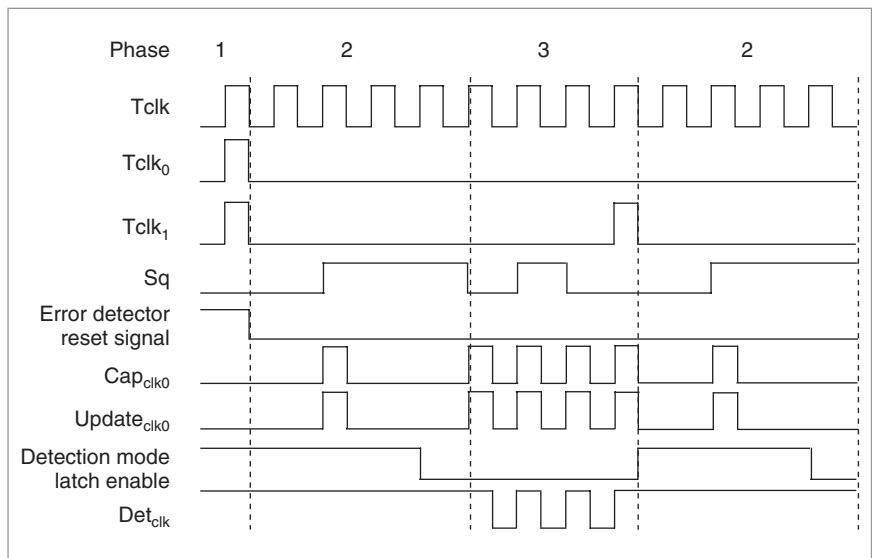


**Figure 5. Timing diagrams for the BIST circuit. For one test pattern, the procedure has three phases: test pattern generation (phase 1), periodic square wave signal port selection and sensitized-path checking (phase 2), and square wave test (phase 3). After the third phase, the procedure returns to the second phase, and the process repeats until the periodic square wave signal for the test pattern has been applied to the last input.**

again to phase 3, and the process continues.

Figure 5 shows timing diagrams for all the signals of

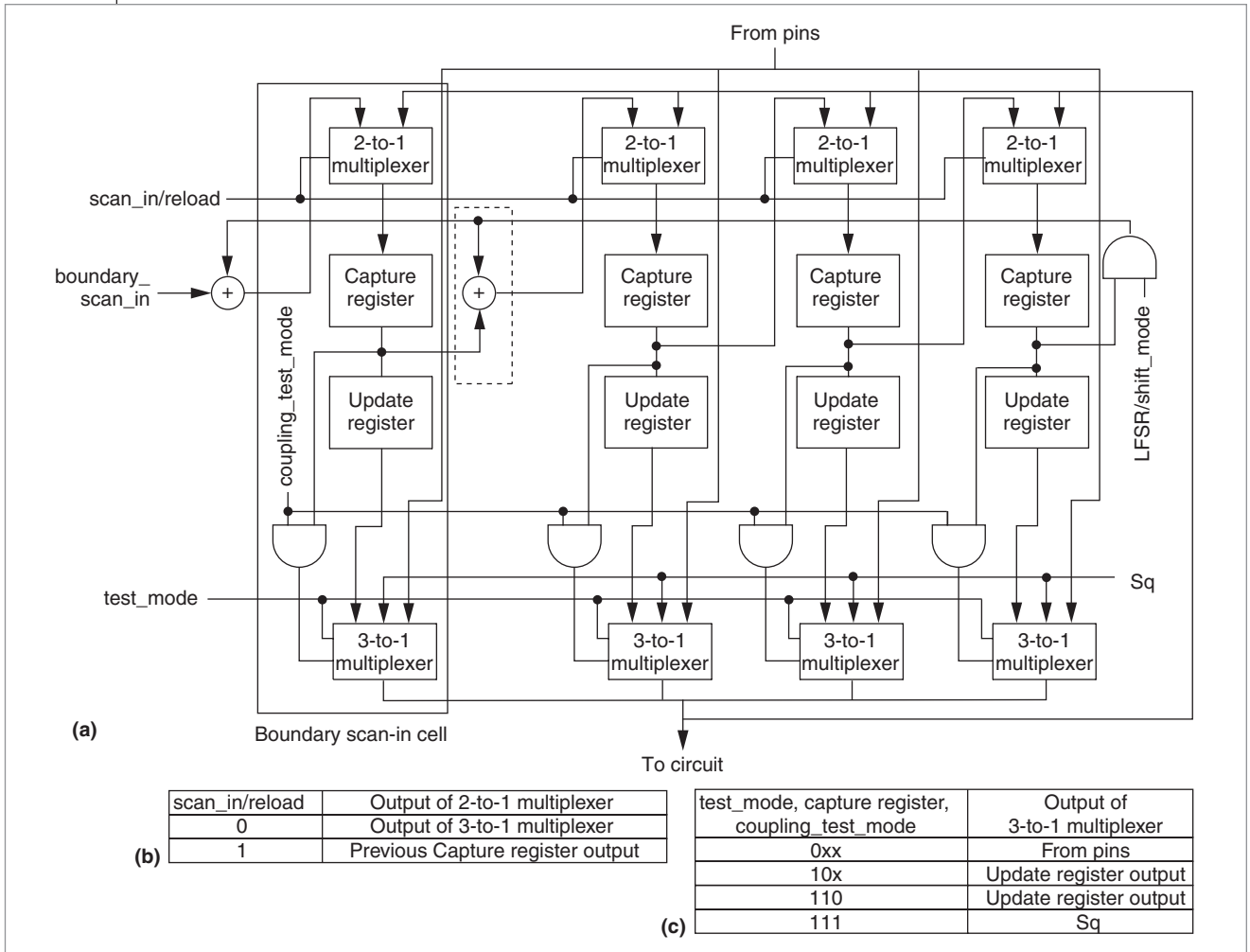


Figure 6. Modified 4-bit boundary scan-in cells (a) and truth tables for the 2-to-1 (b) and 3-to-1 (c) multiplexers.

the test procedure for testing glitches that affect the circuit operation. The circuit operates at the normal speed, and its output data are shifted into DFF<sub>1</sub> and DFF<sub>2</sub>. XOR<sub>1</sub> compares the outputs of DFF<sub>1</sub> and DFF<sub>2</sub>. If the DM latch = 0 (which means the output is not sensitized) but the ED detects a 1, the test has detected an unexpected pulse induced by a crosstalk fault.

In Figure 5, Tclk is the test clock, which can be the CUT's system clock, Cap<sub>clko</sub> and Update<sub>clko</sub> are the capture register and update register signals, respectively, of the boundary scan cell. The circuit can detect the glitches that propagate to DFF<sub>1</sub> when DFF<sub>1</sub> is activated at the rising edge of Cap<sub>clko</sub>. This is the case in which the crosstalk-induced glitches affect the circuit operation in the normal mode. The glitches that arrive before or after the triggering edge of Cap<sub>clko</sub> do not affect the circuit operation and are ignored.

The scheme aims to detect a combinational block's

crosstalk-induced glitch faults. Applying it to a sequential circuit requires the sequential circuit to be scan designed, and we test only the combinational part.

### Boundary scan cell design

For the BIST circuit in Figure 4 to support our test scheme, we need to slightly modify the boundary scan cells.

**Boundary scan-in cell.** The scheme's boundary scan-in cells should be able to implement the LFSR function in addition to the cells' original shifting function. Figure 6 shows the modified 4-bit boundary scan-in cell design with capture and update registers. Each modified boundary scan cell has an added 3-to-1 multiplexer. When transformed into the LFSR mode, the configuration is that of a primitive polynomial  $1 + x + x^4$ . In the first phase, Tclk<sub>0</sub> = 1, and the cells are in the LFSR state,

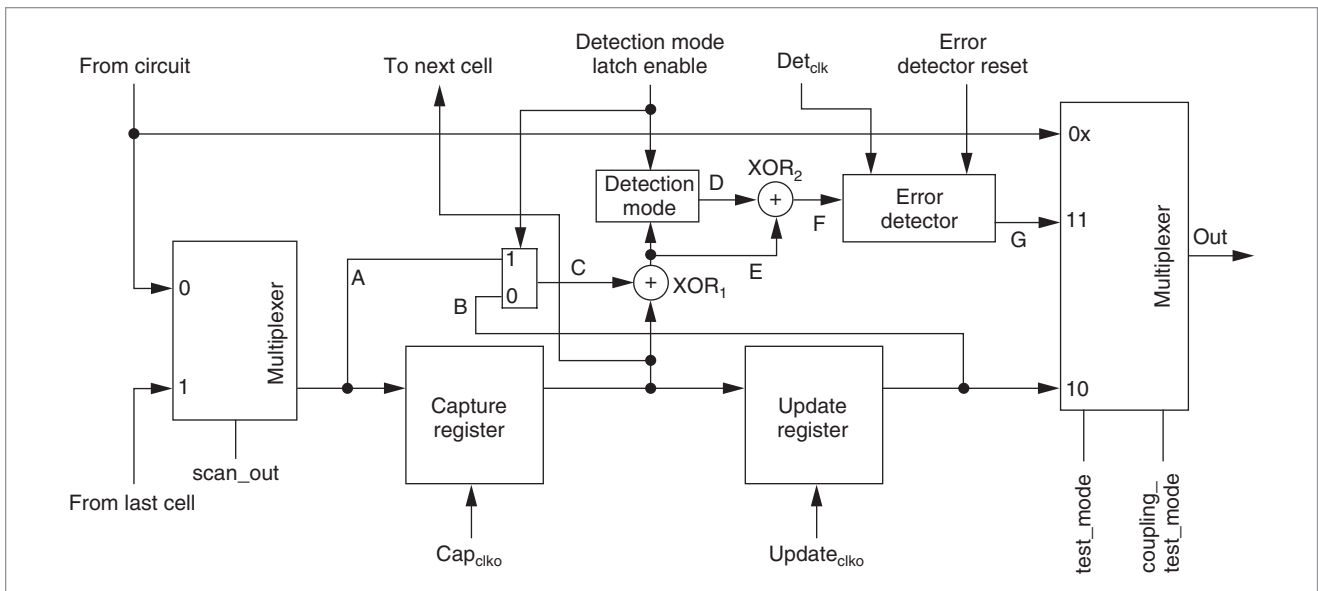


**Figure 7. Modified scan-out cell.**

where LFSR/shift\_mode and scan\_in/reload are set to 1. The capture clock input  $Cap_{clki}$ , which equals  $Tclk_0$  at this moment, starts to clock capture registers until their outputs (the random pattern) are finally stored in update registers when the update clock input ( $Update_{clki}$ ) signal arrives. In the second phase, the capture registers become shift registers, with the LFSR/shift\_mode set to 0. The boundary\_scan\_in, for one test pattern, is set to 1 at the first phase 2 and is set to 0 at the subsequent phase 2. In addition, coupling\_test\_mode and test\_mode are set to 1. The 3-to-1 multiplexer will select  $S_q$  as its input when the corresponding capture clock's output is 1. Figure 6 shows the truth tables for the 2-to-1 and 3-to-1 multiplexers.

When scan\_in/reload is set to 1 and the LFSR/shift\_mode is set to 0, the modified boundary scan-in cells still support the original boundary scan-in function.

**Boundary scan-out cell.** Figure 7 shows in detail the design of the boundary scan-out cell for the detector block. In the figure,  $Det_{clk}$  is the detector clock. EDR is the error detector reset, which resets the error detector (set to 1 in the first phase of the circuit operation) to 0. In the second phase, DMLE is set to 1, an alternating sequence of 1s and 0s is applied to  $S_q$  to check the sensitized output, and a pulse arrives at  $Cap_{clko}$  to capture the first 1 output to be compared with the second 0 output, which appears at line A by XOR<sub>1</sub>. Finally, the DMLE returns to 0. In the third phase, the  $Cap_{clko}$ , the update

clock of the boundary scan-out cell ( $Update_{clko}$ ), and the  $Det_{clk}$  are synchronous with the test clock. The outputs are latched at the capture and update registers at the normal operation speed. XOR<sub>1</sub> compares two consequent outputs and produces a 1 if these two outputs differ.

### Fault coverage estimation through fault simulation

We performed fault simulation to evaluate the fault coverage of the randomly generated patterns for this test scheme.



#### Symbol definition and operation

To perform fault simulation, we first introduce and define a set of symbols to represent the various signals and operation rules for each type of gate. Table 1 defines the set of symbols. Figure 8a shows examples of how these symbols operate through an AND gate. For example,  $C$  and  $C^*$  result in  $PF^*$ , and  $C$  and  $C$  result in  $C$ . Figure 8b shows the truth tables for AND- and OR-gate operation. The tables show that these sets of operations are rather conservative. For example, when  $S$  operates on  $S$  (or  $S^*$ ), an  $x$ , indicating an unknown, while for practical cases, an  $S$  (or  $S^*$ ) most often results.

#### Fault simulation

The first step for fault simulation is to compute the logic values for the fault-free circuit using the set of variables and operation rules defined in Table 1 and Figure 8. The paths with the  $S$  signal are sensitized paths. Then a

Table 1. Symbols for square wave tests.

Symbol	Representation
0	Static 0
1	Static 1
C*	Fault effect signal with positive pulse at logic 0 
C	Fault effect signal with negative pulse at logic 1 
PF*	Potential fault effect signal, either 0 or C*
PF	Potential fault effect signal, either 1 or C
S*	Complement of signal S without considering the timing issue
S	Periodic square wave signal
x	Don't care

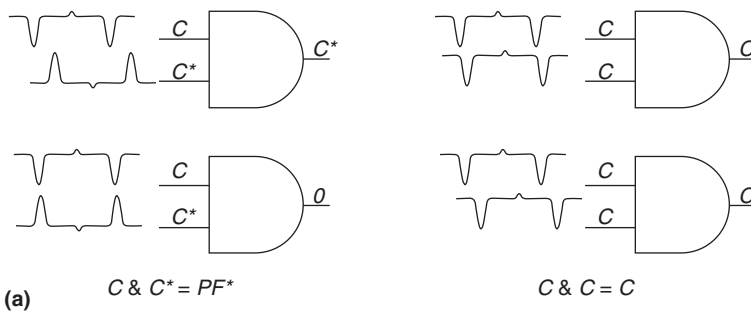
the simulator moves on to another pattern.

Experimental results

Figure 9 shows the simulation results of the modified boundary scan-out cell of Figure 7 under the timings of Figure 5. In Figure 9, clock signal Tclk, square wave test signal Sq, and control signals DMLE and Det<sub>clk</sub> (for the DM latch and the ED) appear with the simulated signals at FC (the input of the cell where the induced glitches occur), F (XOR<sub>2</sub>'s output), and Out (the boundary cell detector's output). When DMLE is high (that is, the circuit is at the stable logic latch phase, for which Det<sub>clk</sub> is high), even if there is an induced glitch at FC (at 3.3 ns), the DM latch

doesn't detect the glitch and the boundary cell output is low. When DMLE is low (the square wave test phase), if the glitch occurs at the time slot when Det<sub>clk</sub> is low (at 7 ns), the circuit detects it and the output is high.

To estimate the random test patterns' efficiency in detecting crosstalk faults, we randomly generated patterns to apply to benchmark circuits<sup>13</sup> into which we randomly injected crosstalk faults. We implemented a fault simulator based on our symbols and operation rules to evaluate the fault coverage. For each circuit, we generated two nonoverlapping sets of random crosstalk faults; the number of faults was twice the number of gates. For each fault set, we generated two separate sets of random patterns, each with a different seed for



	0	1	C*	C	PF*	PF	S*	S	x
0	0	0	0	0	0	0	0	0	0
1	0	1	C*	C	PF*	PF	S*	S	x
C*	0	C*	0	PF*	PF*	PF*	x	x	x
C	0	C	PF*	C	PF*	C	x	x	x
PF*	0	PF*	PF*	PF*	PF*	PF*	x	x	x
PF	0	PF	PF*	C	PF*	PF	x	x	x
S*	0	S*	x	x	x	x	x	x	x
S	0	S	x	x	x	x	x	x	x
x	0	x	x	x	x	x	x	x	x

	0	1	C*	C	PF*	PF	S*	S	x
0	0	1	C*	C	PF*	PF	S*	S	x
1	1	1	1	1	1	1	1	1	1
C*	C*	1	C*	PF	C*	PF	x	x	x
C	C	1	PF	1	PF	PF	x	x	x
PF*	PF*	1	C*	PF	PF*	PF	x	x	x
PF	PF	1	PF	PF	PF	PF	x	x	x
S*	S*	1	x	x	x	x	x	x	x
S	S	1	x	x	x	x	x	x	x
x	x	1	x	x	x	x	x	x	x

(b) AND-gate OR-gate

Figure 8. Examples of AND operation on symbols C and C\* (a); operation tables for symbols for AND and OR gates (b).

coupling crosstalk fault is injected. If the aggressor line of the crosstalk fault is at one of S (oscillating) paths, the fault site's victim line is set to C. If this C propagates toward the circuit's outputs, the propagation is successful, the pattern detects the crosstalk fault, and another fault is injected. This process repeats, eventually injecting all faults; then

pattern generation.

Table 2 (p. 168) shows results for benchmark circuits, where c represents the combinational part of the circuit. Saturated fault coverage depends strongly on the circuit type. For example, for circuits C5315, S13207c, S15850c, and S35932c, which are mainly large



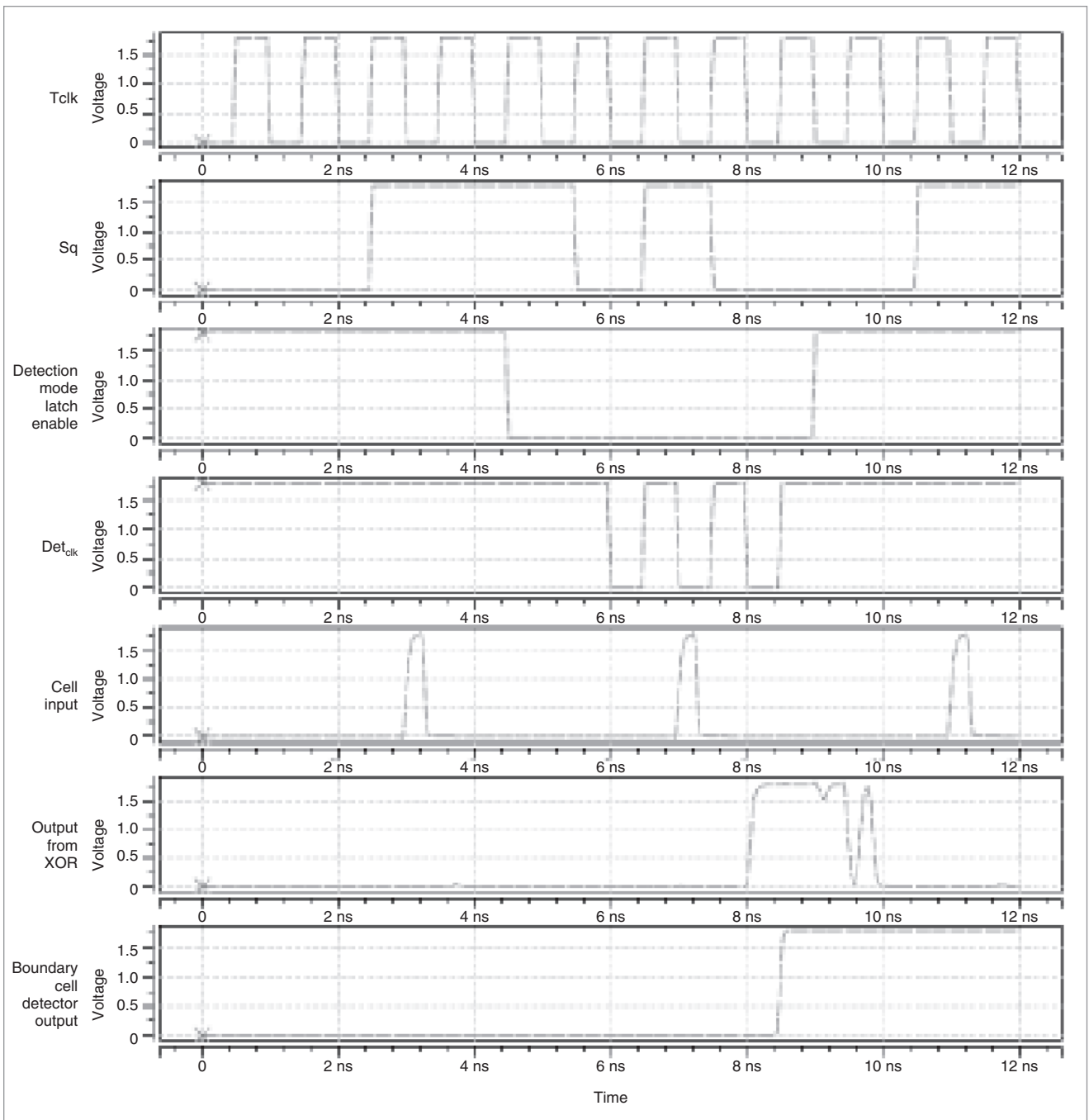


**Figure 9. Hspice simulation waveforms for the modified boundary scan-out cell in Figure 7.**

circuits, it can easily reach 90%; for circuit C6288, which is a multiplier, it reaches only 30%. Also, because of their random selection, some of the faults might be untestable. Fault coverage also depends somewhat on the set of random test patterns, which are generated with different LFSR seeds. However, the difference in fault coverage between two sets of patterns is generally small—within 2%. This means that for an arbitrary set

of random patterns, the BIST scheme can detect crosstalk faults quite efficiently, making it very attractive in a practical application.

Table 2 compiles detailed simulation results. The total number of (randomly selected) faults for each circuit is twice the number of gates. The “no. of patterns to reach saturation” column shows the number of random patterns that have been generated by the software LFSR



Table 2. Fault simulation results for the proposed BIST scheme.

Circuit name	Total no. of primary inputs	Total no. of faults	No. of patterns to reach saturation	Saturated coverage fault (percentage)	Potential detectable fault coverage (percentage)
C2670	157	2,700	2,700	69.07	7.11
C3540	50	3,438	3,426	83.33	8.20
C5315	178	4,970	4,899	94.81	2.90
C6288	32	4,896	3,741	28.82	13.01
C7552	206	7,436	3,896	90.14	3.28
S3271c	142	3,428	2,430	97.52	0.90
S3330c	172	3,922	3,879	79.40	0.33
S3384c	209	3,788	2,352	93.98	0.37
S4863c	153	4,990	4,115	94.71	0.54
S5378c	214	5,986	3,918	97.24	0.60
S6669c	312	6,784	1,643	98.28	0.25
S9234c	247	11,688	1,718	83.10	0.48
S13207c	650	17,202	436	92.34	0.11
S15850c	600	20,744	419	92.98	0.10
S35932c	1,763	35,656	87	96.85	0.44
S38584c	1,462	41,430	94	90.61	1.51

when the fault coverage reached the saturated value, shown in the “saturated fault coverage” column. “Potential detectable fault coverage” is the fault coverage when one or more *PFs* or *PFs\** is detected at the circuit output(s). The table shows that for most circuits, the saturated fault coverage can exceed 90%, with fewer patterns than faults.

**THIS ARTICLE** demonstrated a scheme that makes it simple to detect crosstalk faults in deep-submicron VLSI circuits in the boundary scan environment. These faults are difficult to detect by other means. Our BIST scheme is easy to implement and requires minimal modification of the boundary scan cells for the circuit. Simulation results show that with a small number of random patterns for most large circuits, the scheme can detect most crosstalk faults, with fault coverage reaching or exceeding 90%.

## References

1. TSMC 0.18um Mixed Signal 1P6M salicide 1.8/3.3v RF SPICE models, Taiwan Semiconductor Manufacturing Corp., 2004; <http://www.tsmc.com.tw>.
2. W. Chen, S.K. Gupta, and M.A. Breuer, “Analytic Model for Crosstalk Delay and Pulse Analysis Under Non-Ideal Inputs,” *Proc. IEEE 1997 Int’l Test Conf. (ITC 97)*, IEEE CS Press, 1998, pp. 809-818.
3. K.T. Lee, C. Nordquist, and J.A. Abraham, “Automatic Test Pattern Generation for Crosstalk in Digital Circuits,” *Proc. 16th IEEE VLSI Test Symp. (VTS 98)*, IEEE CS Press, 1998, pp. 34-39.
4. P.B. Sabet and F. Ilpouse, “A Model for Crosstalk Noise Evaluation in Deep Submicron Processes,” *Proc. 2nd Int’l Symp. Quality Electronic Design (ISQED 01)*, IEEE CS Press, 2001, pp. 139-144.
5. A. Rubio et al., “An Approach to the Analysis and Detection of Crosstalk Faults in Digital VLSI Circuits,” *IEEE Trans. Computer-Aided Design of Integrated Circuits and Systems*, vol. 13, no. 3, Mar. 1994, pp. 359-369.
6. N. Itazaki, Y. Idomoto, and K. Kinoshita, “A Fault Simulation Method for Crosstalk Faults in Synchronous Sequential Circuits,” *Proc. 26th Int’l Symp. Fault-Tolerant Computing (FTCS 96)*, IEEE CS Press, 1996, pp. 38-43.
7. Y. Zhao and S. Dey, “Analysis of Interconnect Crosstalk Defect Coverage of Test Sets,” *Proc. IEEE Int’l Test Conf. (ITC 00)*, IEEE CS Press, 2000, pp. 492-501.
8. X. Bai, S. Dey, and J. Rajski, “Self-Test Methodology for At-Speed Test of Crosstalk in Chip Interconnects,” *Proc. 37th Design Automation Conf. (DAC 00)*, ACM Press, 2000, pp. 614-624.
9. W.C. Lai, J.R. Huang, and K.T. Cheng, “Embedded-Software-Based Approach to Testing Crosstalk-Induced Faults at On-Chip Buses,” *Proc. 19th IEEE VLSI Test*

Symp. (VTS 01), IEEE CS Press, 2001, pp. 204-209.

10. W.Y. Chen, S.K. Gupta, and M.A. Bruer, "Test Generation for Crosstalk-Induced Faults: Framework and Computational Results," *Proc. 9th Asian Test Symp. (ATS 00)*, IEEE CS Press, 2000, pp. 305-310.
11. M.S. Wu et al., "A Testing Scheme for Crosstalk Faults Based on the Oscillation Test Signal," *Proc. 11th Asian Test Symp. (ATS 02)*, IEEE CS Press, 2002, pp. 170-175.
12. F. Brglez, D. Bryan, and K. Kozminski, "Combinational Profiles of Sequential Benchmark Circuits," *Proc. IEEE Int'l Symp. Circuits and Systems (ISCAS 89)*, IEEE Press, 1989, pp. 1929-1934.
13. M. Cuviallo et al., "Fault Modeling and Simulation for Crosstalk in System-on-Chip Interconnects," *Proc. Int'l Conf. Computer-Aided Design (ICCAD 99)*, IEEE CS Press, 1999, pp. 297-303.



**Ming Shae Wu** is a PhD student in the Department of Electronics Engineering at National Chiao Tung University, Taiwan. His main research interest is deep-submicron VLSI testing. Wu

has a BS and an MS, all in electronics engineering from National Chiao Tung University.



**Chung Len Lee** is a faculty member in the Department of Electronics Engineering at National Chiao Tung University, Taiwan. His research interests include IC design, CAD, and testing.

Lee has a BS from National Taiwan University and an MS and PhD from Carnegie Mellon University, all in electrical engineering. He is a senior member of IEEE Computer Society.

■ Direct questions and comments about this article to Chung Len Lee, Department of Electronics Engineering, National Chiao Tung University, Hsin Chu, Taiwan, [cllee@mail.nctu.edu.tw](mailto:cllee@mail.nctu.edu.tw).

For further information on this or any other computing topic, visit our Digital Library at <http://www.computer.org/publications/dlib>.

## IEEE Design & Test Call for Papers

*IEEE Design & Test*, a bimonthly publication of the IEEE Computer Society and the IEEE Circuits and Systems Society, seeks original manuscripts for publication. *D&T* publishes articles on current and near-future practice in the design and test of electronic-products hardware and supportive software. Tutorials, how-to articles, and real-world case studies are also welcome. Readers include users, developers, and researchers concerned with the design and test of chips, assemblies, and integrated systems. Topics of interest include

- Analog and RF design,
- Board and system test,
- Circuit testing,
- Deep-submicron technology,
- Design verification and validation,
- Electronic design automation,
- Embedded systems,
- Fault diagnosis,
- Hardware/software codesign,
- IC design and test,
- Logic design and test,
- Microprocessor chips,
- Power consumption,
- Reconfigurable systems,
- Systems on chips (SoCs),
- VLSI; and
- Related areas.

To submit a manuscript to *D&T*, access Manuscript Central, <http://cs-ieee.manuscriptcentral.com>. Acceptable file formats include MS Word, PDF, ASCII or plain text, and PostScript. Manuscripts should not exceed 5,000 words (with each average-size figure counting as 150 words toward this limit), including references and biographies; this amounts to about 4,200 words of text and five figures. Manuscripts must be doubled-spaced, on A4 or 8.5-by-11 inch pages, and type size must be at least 11 points. Please include all figures and tables, as well as a cover page with author contact information (name, postal address, phone, fax, and e-mail address) and a 150-word abstract. Submitted manuscripts must not have been previously published or currently submitted for publication elsewhere, and all manuscripts must be cleared for publication.

To ensure that articles maintain technical accuracy and reflect current practice, *D&T* places each manuscript in a peer-review process. At least three reviewers, each with expertise on the given topic, will review your manuscript. Reviewers may recommend modifications or suggest additional areas for discussion. Accepted articles will be edited for structure, style, clarity, and readability. Please read our author guidelines (including important style information) at <http://www.computer.org/dt/author.htm>.

**Submit your manuscript to *IEEE Design & Test* today!**

*D&T* will strive to reach decisions on all manuscripts within six months of submission.

IEEE  
**Design & Test**  
of Computers